Inorganica Chimica Acta 520 (2021) 120274

Contents lists available at ScienceDirect

Inorganica Chimica Acta

journal homepage: www.elsevier.com/locate/ica

Research paper

Anionic 1-Aza-3,4-diphospholides as redox active ligands

Riccardo Suter [a], Robert J. Gilliard [b], Javad Iskandarov [c], Zoltan Benkő [c,*], Michael Wörle [a], Hansjörg Grützmacher [a,*]

[a] Department of Chemistry and Applied Biosciences, ETH Zurich, CH-8093 Zurich, Switzerland
[b] Department of Chemistry, University of Virginia, Charlottesville, VA 22904-4319, United States
[c] Budapest University of Technology and Economics, Szent Gellért tér 4, 1111 Budapest, Hungary

ARTICLE INFO

Keywords:
Phosphorus heterocycles
Polyphosphanes
Iron complexes
Redox Chemistry
Metal metal bonds

ABSTRACT

Herein we present the redox active behaviour of the sodium salt of 1-aza-3,4-diphospholide Na[**1**]. Cyclic voltammetry in MeCN shows an irreversible reduction and an irreversible oxidation wave indicating EC mechanisms. This anionic heterocycle is chemically oxidized with hexachloroethane likely to a short-lived 1-aza-3,4-diphospholyl radical which rapidly dimerizes to give bis(1-aza-3,4-diphospholyl) (**2**) which contains a tetraphosphane unit, P—P—P—P. In solution and in the solid state a *rac*- and *meso*-isomer have been identified. The oxidation reaction is chemically reversible, and using lithium metal, the central P—P bond in **2** can be cleaved to afford Li[**1**]. Both the anion [**1**]$^-$ and the P—P coupled dimer **2** have been applied as ligands in combination with iron carbonyl precursors to isolate the strawberry red complex [FeCp(η^1-**1**)(CO)$_2$] (**3**). This complex undergoes dimerization under the loss of carbon monoxide to form the complex [Fe$_2$(Cp)$_2$(μ_2-**1**)(CO)$_2$] (**4-syn** and **4-anti**). The reaction of bis(1-aza-3,4-diphospholyl) **2** with [Fe$_3$(CO)$_{12}$] in THF leads to cleavage of the P—P bond, and a dinuclear complex [Fe$_2$(μ_2–**1**)$_2$(CO)$_6$] (**5**) with a direct Fe(I)—Fe(I) bond [Å = 2.5866(4)] is obtained.

1. Introduction

1,3,4-triphospholes are accessible via a variety of synthetic routes from phosphaalkynes [1,2] or phosphaketenes [3] and show versatile binding modes in transition metal complexes [4,5]. Furthermore the formation of iron or copper containing coordination polymers has been reported [6,7]. Upon oxidation, these phosphorus rich molecules tend to form cage compounds [8–11]. An exception is the 1H-1,2,4-triphosphole **I** which dimerizes upon addition of water resulting in the formation of a P—P dimer **II** (Scheme 1). This dimer undergoes a homolytic P—P bond dissociation reaction to form two stable triphosphole radicals [12]. The dinitrogen analogue 1,2-diaza-4-phospholide [**III**]$^-$ undergoes an oxidative coupling reaction to form the P—N coupled dimer **IV** [13] which can be reduced to its dipotassium radical complex [14]. The diazaphospholide [**III**]$^-$ shows a rich coordination chemistry with alkali metals, lanthanides and transition metals [15–19], and it has been employed as a ligand to stabilize Bi-Bi and Sb-Sb bonds [20,21]. We recently reported a new 1-aza-3,4-diphospholide Na[**1**] [22] and their annulated analogues [23]. They can be synthesized from two equivalents of Na(OCP) [24–28] and imidoyl chlorides in a mechanism which is accompanied by the loss of carbon monoxide [29]. This anionic heterocycle is the structural link between the 1,3,4-triphospholides and the 1,2-diaza-4-phospholides (Scheme 1). Herein, we report the redox chemistry of the 1-aza-3,4-diphospholide salts and its coordinating behaviour in iron complexes.

2. Results

Structural and theoretical investigations have shown that the easily accessible 1-aza-3,4-diphospholide anion [**1**]$^-$ is electron rich, highlighted with an energetically high lying HOMO in a model compound Na[**1′**] (Fig. 1). To gain insight into the redox activity of anion [**1**]$^-$ and to provide a deeper understanding on its electronic properties, cyclic voltammetry (CV) measurements were performed ((for details consult the Supporting information). In acetonitrile, an oxidation at −0.58 V and reduction wave at −1.72 V against the Fc/Fc$^+$ couple as standard were observed (Fig. 1). The separation of the oxidation and reduction peak potentials by 1.04 V indicates an irreversible electrochemical redox-process in which a chemical reaction might be involved (EC mechanism). This inspired us to scrutinize the chemical oxidation of anion [**1**]$^-$. The anionic azadiphospholide Na[**1**] was therefore mixed with half an equivalent of hexachloroethane which led to an immediate

* Corresponding authors.
E-mail addresses: zbenko@mail.bme.hu (Z. Benkő), hgruetzmacher@ethz.ch (H. Grützmacher).

https://doi.org/10.1016/j.ica.2021.120274
Received 6 December 2020; Received in revised form 20 January 2021; Accepted 20 January 2021
Available online 4 February 2021

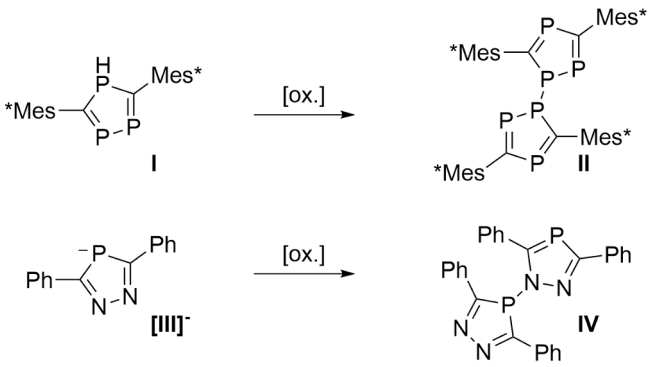

Scheme 1. Triphospholes **I** and diazaphospholides $[\mathbf{III}]^-$ oxidatively couple to form dimers **II** and **IV**, respectively.

colour change of the reaction mixture from colourless to dark yellow (Scheme 2).

According to the UV/VIS spectra, the process is accompanied by a significant bathochromic shift of 35 nm (λ_{max} from 372 nm to 407 nm). The ^{31}P NMR spectrum of the reaction mixture indicated a clean formation of two similar species having complex and partially overlapping multiplet resonances (Fig. 1). To resolve these multiplet resonances, low temperature (263 K) ^{31}P NMR measurements in C_6D_6 were carried out. The data were analysed and resulted in the elucidation of two AA′XX′ spin systems corresponding to two stereoisomeric structures (vide infra): one at δ (ppm) = -39.2 (m), 75.4 (m) with $^1J_{AA'} = 305.2$ Hz, $^3J_{XX'} = 34.4$ Hz, $^1J_{AX} = 310.6$ Hz, $^2J_{AX'} = 9.6$ Hz and another at δ (ppm) = −48.2 (m), 74.3 (m) with $^1J_{AA'} = 239.6$ Hz, $^1J_{AX} = 300.0$ Hz, $^2J_{AX'} = -9.5$ Hz, $^3J_{XX'} = 0$ Hz. These multiplets are consistent with the formation of P—P bonded dimeric species, resembling the spectra obtained for other P_4-chain type arrangements [30–39].

It may be anticipated that the initially formed single electron oxidation product is a short-lived 1-aza-3,4-diphospholyl radical with the spin density mainly localized at the P center, which rapidly dimerizes to form a P—P bond. This is in line with the large contribution of one of the P atoms in the HOMO of the model compound Na[**1'**] shown in Fig. 1. We were interested in whether the bis(1-aza-3,4-diphospholyl) **2** can be reduced back to anion $[\mathbf{1}]^-$ and based on the results of the CV measurements this reduction may be possible using alkali metals. To achieve this, a solution of **2** in DME was stirred overnight with an excess of lithium (Scheme 2). ^{31}P NMR spectroscopic investigations revealed a clean and quantitative reduction of **2** back to the anion $[\mathbf{1}]^-$. From a saturated hexane solution at −30 °C, yellow crystals of the dimer **2** can be isolated. Since selective crystallisation of one isomer was not possible (and hence an exact assignment of the NMR data is likewise not possible) several crystals were mounted to obtain the solid state structures of both diasteromers **2-meso** and **2-rac** (Fig. 2). Both diasteromers contain bridgehead phosphorus atoms which have a pyramidalized coordination sphere (sum of angles around P1 and P3 in **2-rac** 292.2° and 298.7 and in **2-meso** 287.0° and 280.7°, respectively). The CO bond distances (1.214 – 1.233 Å) in the dimers are significantly shorter than in the monomeric azadiphospholide anions $[\mathbf{1}]^-$ (1.266 – 1.282 Å) which is consistent with the increased double bond character of the C—O bond in **2** compared to the alkoxide moiety in $[\mathbf{1}]^-$.

In **2**, the C1 P1 bond distance (1.824 – 1.856 Å) matches a typical C—P single bond, while the C2 P2 bond length (1.705 – 1.720 Å) is similar to the one in $[\mathbf{1}]^-$ (1.713–1.724 Å) and can also be considered a C═P double bond. This supports a description with localized bonds for the two bridged azadiphosphole moieties. The endocyclic P—P bonds (ca. 2.17 Å) are somewhat shorter than the bridging ones (ca. 2.23 Å, in the range of a normal P—P single bond) [40] indicating only a small delocalization in the azadiphosphole unit. The bond distances in **2** are significantly longer than the P—P dimer of 1H-1,2,4-triphosphole **II** (bridging P—P bond 2.17 Å; endocyclic P—P bond 2.12 Å). The C═P bond lengths (1.72–1.78 Å), however, do not differ significantly.

To study the coordination properties of the azadiphospholide Na[**1**],

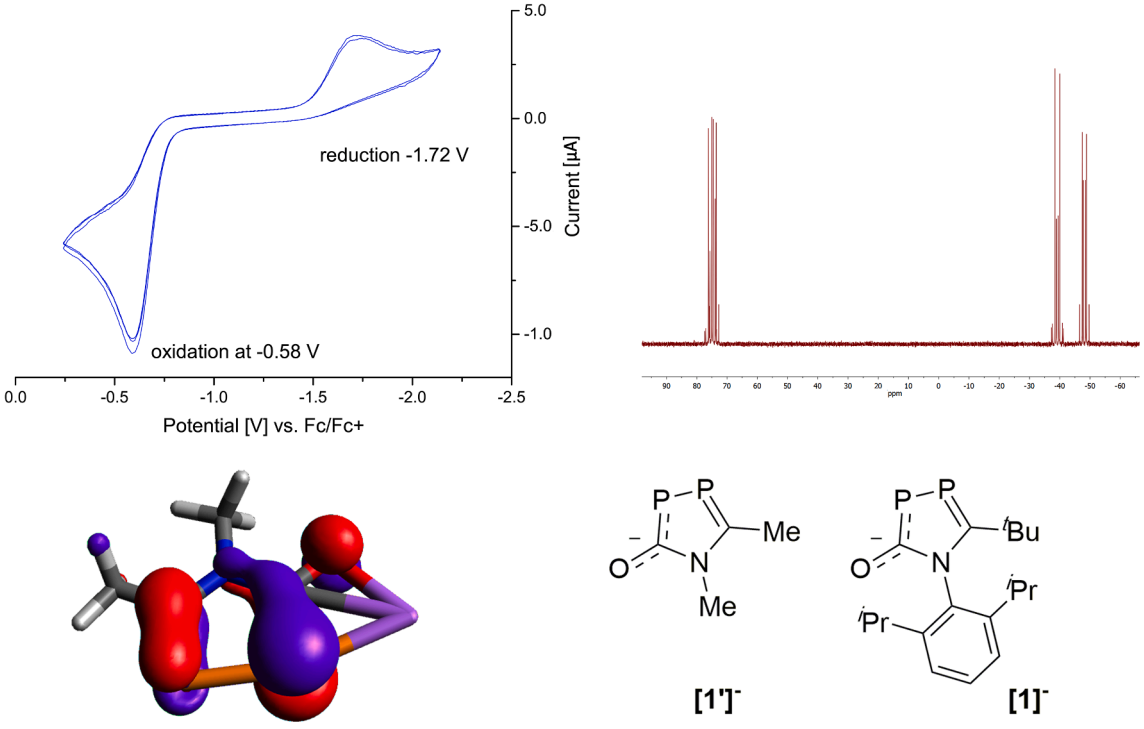

Fig. 1. (*top left*): Cyclic voltammogram of Na[**1**] in MeCN 200 mV/s with $(NBu_4)PF_6$ oxidized at −0.58 V and reduced at −1.72 V. (*top right*): ^{31}P NMR spectrum of the P_4-chains **2-rac** and **2-meso** in a C_6D_6 solution. (*bottom*) the HOMO orbital of the ion pair in the model compound Na[**1**′], where the DIP substituent at nitrogen is substituted with a Me group and the *t*Bu at the carbon atom is replaced by Me with a contour value of 0.05 (DFT, BP86/cc-pVDZ) (The sodium counter ion is shown in purple with contacts to the P, C, and O atom).

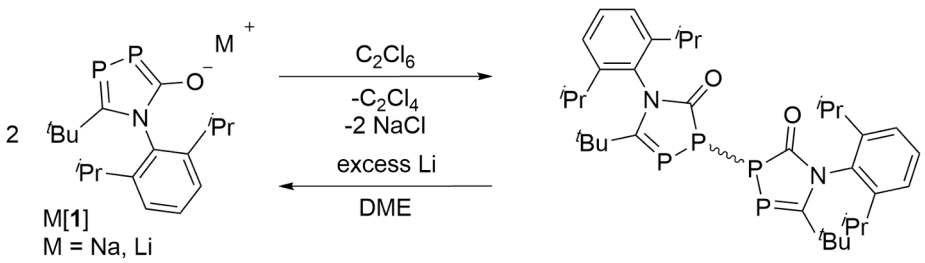

Scheme 2. One electron oxidation of azadiphospholide Na[**1**] leading to the tetraphosphanes **2-rac** and **2-meso**. This mixture can be reduced with lithium to form Li[**1**].

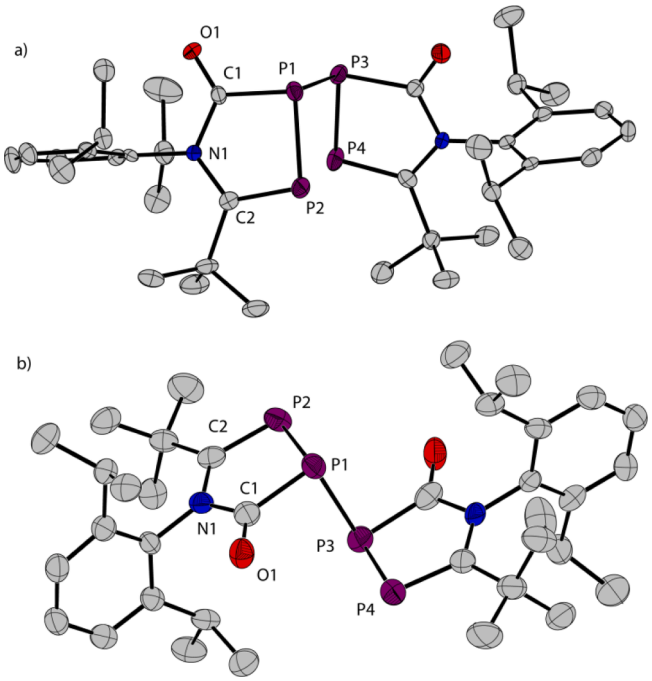

Fig. 2. P_4-chains **2-rac** (a) and **2-meso** (b). Anisotropic thermal displacement ellipsoids are shown at the 50% probability level. Hydrogen atoms and solvent molecules are omitted for clarity. **2-rac** interatomic distances (Å): P1 P2 2.1684 (13), P1 P3 2.2328(13), P1 C1 1.850(3), P2 C2 1.720(3), P3 P4 2.1713(13), P3 C19 1.856(4), P4 C20 1.713(3), O1 C1 1.216(4), O2 C19 1.214(4), N1 C1 1.401 (4), N1 *C2* 1.403(4), N2 C19 1.405(4), N2 C20 1.412(4) **2-meso** interatomic distances (Å): P1 P2 2.175(2), P1 P3 2.231(2), P1 C1 1.824(6), P2 C2 1.713(5), P3 P4 2.174(2), P3 C19 1.845(6), P4 C20 1.705(5), O1 C1 1.233(6), O2 C19 1.230(6), N1 C1 1.400(7), N1 C2 1.417(7), N2 C19 1.406(7), N2 C20 1.422(6).

a THF solution of the anion was added to the iron precursor [Fe(Cp)(I)$(CO)_2$] (FpI) in THF, resulting in a colour change of the reaction mixture from brown to strawberry red. The ^{31}P NMR spectrum of the reaction mixture contained one pair of doublet resonances at $\delta = -57.7$ and 113.7 ppm with a coupling of $^1J_{P,P} = 333$ Hz. Compared to the anionic 1,3,4-azadiphospholide Na[**1**] ($^1J_{P,P} = 393$ Hz), the $^1J_{P,P}$ coupling constant is significantly smaller, which indicates a η^1-coordination of the phosphole through the phosphorus atom which involves a change from a λ_3-σ_2-P to a λ_3-σ_3-P donor atom. In the solid state, three carbonyl bands (ν_{CO} = 2021, 1990 and 1966 cm^{-1}) are observed in the IR spectrum which exclude a η^5-coordination mode of the 1,3,4-azadiphospholide and the formation of a phospha-ferrocene type complex which would not show any CO stretching vibrations [41]. In addition to the strong metal carbonyl frequencies, a C═O vibration band is observed at 1578 cm^{-1}, which is assigned to the C═O group of the azadiphosphole. This supports the assumption that compound **3** contains a η^1-phosphorus-bonded azadiphospholide ring and can be formulated as [Fe(Cp)(η^1-**1**)$(CO)_2$]. The structurally related complex **V** shows likewise a η^1-coordination of the phosphorus heterocycle (Scheme 3) and exhibits similar IR spectroscopic features (ν_{CO} = 2015, 1970 cm^{-1}) [41].

Single crystal X-ray diffraction analysis allowed us to unambiguously confirm the structure of complex **3** (Fig. 3). The azadiphospholide binds through the P1 atom, which is in a pyramidalized coordination sphere (sum of angles at the phosphorus atom of 318.9°). The FeP bond length (2.2919(8) Å) is in the typical range for terminal iron phosphide bonds, Fe PR_2 (2.265 Å) [42]. The C═O group of the azadiphosphole is rather short [1.230(3) Å], a strong indication for a C═O double bond. The oxygen atom is pointing away from the iron center (FeO 3.732 Å) and excludes a possible η^3-coordination with P1, C1 and O1. The same product has been observed in the reaction of the compound **2** with one equivalent of the Fp-dimer ([$Fe_2(Cp)_2(CO)_4$]) after stirring in toluene at 50 °C for 16 h. In this reaction, the central P—P bond in **2** is reductively cleaved into two azadiphosphole units under concomitant oxidation of the Fe(I) to Fe(II). At first glance it may be surprising that the iron centre is bound to the phosphorus atom in complex **3** because iron is rather oxophilic and its coordination at the oxygen centre would lead to a 6π electron aromatic configuration within the azadiphospholide ring. Anion [**1**]$^-$ shows ambident properties as seen in the HOMO of Na[**1'**] in Fig. 1, which shows the largest contribution at the P1 centre adjacent to the CO unit, while the O atom is more negatively charged (NPA charges at the BP86/cc-pVDZ level −0.79 e at the O and −0.25 e at the P center). The relative energies between **3'** and its structural isomer with Fe coordinating at the O centre were determined by DFT calculations which show that the latter lies significantly higher in energy by 16.0 kcal/mol in agreement with the experiment. Note that the calculated homolytic bond dissociation energies, 47.0 kcal/mol for Fe-P and 67.7 kcal/mol for Fe-O, would suggest the preference of Fe coordination to the oxygen center. This contradiction can be resolved by considering the high stability of the C═O bond (99.5 kcal/mol) in contrast to that of the P═C bond (50.4 kcal/mol). Thus, the formation of complex **3'** is clearly preferred over its isomer, because the stability of the CO π-bond compared to that of the PC π-bond overrules the difference between the Fe-P and Fe-O bond strengths.

Complex **3** can be stored under an argon or nitrogen atmosphere as a solid without noticeable decomposition for several months. But if a THF solution of **3** is exposed to sunlight for 6 days, the deep red colour vanishes and a dark yellow solution is obtained. The ^{31}P NMR spectrum of the solution reveals the complete conversion of the starting material, while three new compounds have been formed. The major compound consists of four non-magnetically equivalent phosphorus atoms coupling to each other; ^{31}P NMR (THF, 121.5 MHz): δ (ppm) = 136.4 (ddd, $J_{P,P}$ = 24, 52, 281 Hz), 122.8 (ddd, $J_{P,P}$ = 6, 24, 382 Hz), 3.8 (ddd, $J_{P,P}$ = 6, 26, 281 Hz), −36.3 (ddd, $J_{P,P}$ = 26, 52, 382 Hz). After another 7 days, the signals of this species vanishes and converts cleanly to the two other products. The reaction can be accelerated using a medium pressure mercury UV lamp, which shortens the reaction time to 3 h. The multiplets of the two final products have been simulated and fitted to the original spectra; ^{31}P{^{1}H} NMR (THF, 121.5 MHz): δ (ppm) = 133.6 (m), −77.8 (m) [$^1J_{AA'}$ = 124.6 Hz, $^3J_{XX'}$ = 0 Hz, $^1J_{AX}$ = 308.7 Hz, $^2J_{AX'}$ = −15.8 Hz] and ^{31}P{^{1}H} NMR (THF, 121.5 MHz): δ (ppm) = 123.8 (m), −77.9 (m) [$^1J_{AA'}$ = 137.7 Hz, $^3J_{XX'}$ = 0 Hz, $^1J_{AX}$ = 314.4 Hz, $^2J_{AX'}$ = 4.8

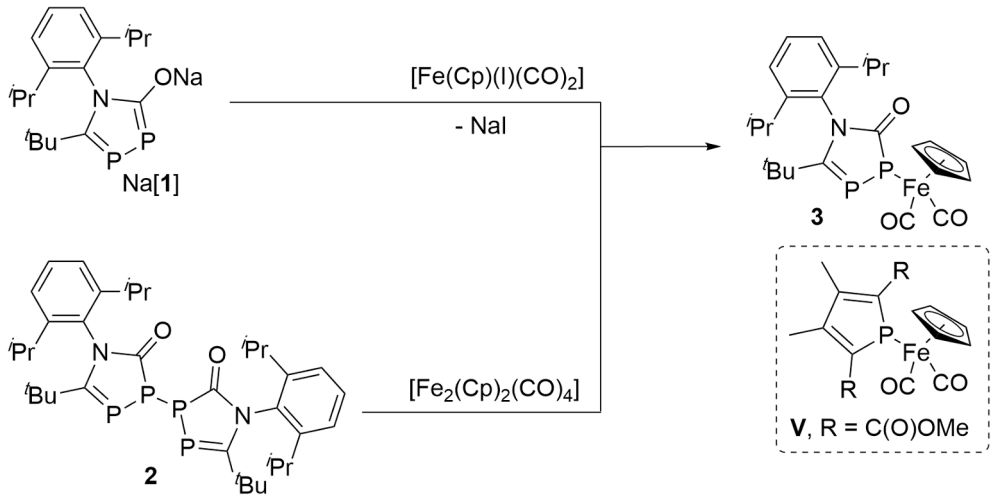

Scheme 3. Formation of mononuclear iron complex [FeCp(η^1-**1**(P))$(CO)_2$] **3** from Na[**1**] and [Fe(Cp)(I)$(CO)_2$] or from **2** with [$Fe(Cp)_2(CO)_4$] compared to the related complex **V**.

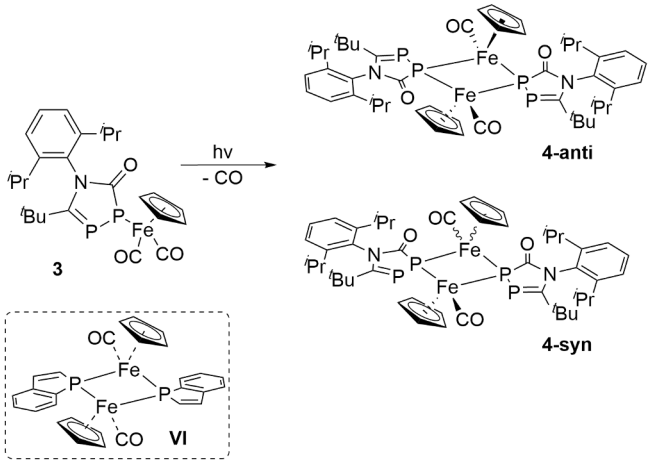

Scheme 4. Iron complex **3** loses carbon monoxide to from the two diasteromers [$Fe_2(Cp)_2(\mu_2$–**1**$)(CO)_2$] **4-anti** and **4-syn** similar to compound **VI**. [43]

Hz]. Two types of red crystals were isolated from a benzene-ether solution by slow evaporation of the solvent each containing dinuclear iron complexes with the formula [$Fe_2(Cp)_2(\mu_2$–**1**$)(CO)_2$]. Selective crystallization of either **4-syn** or **4-anti** was not possible and both compounds are obtained simultaneously in form of differently shaped single crystals. One of those contains only **4-anti** in which the two cyclopentadienyl groups are pointing to different sites of the central planar Fe_2P_2 ring - the midpoint of which corresponds to the inversion center of the molecule. The other crystal contains the two isomers of **4-syn** which results in a disorder around the iron center. The central Fe_2P_2 ring of **4-syn** is slightly folded [Θ = 20.6366(7) °]. The Fe Fe distance in both compounds is above 3.4 Å and excludes any interaction between the metal centers. The P1 phosphorus atom of the azadiphospholide bridges two iron centres which are bound to one remaining carbon monoxide (Fig. 4). The Fe P distances (average 2.261 Å) are very slightly shortened with respect to the Fe P distance in the mononuclear complex **3** which is typical for μ_2-bridging iron phosphide complexes [42]. The other bond distances are similar compared to the ones observed in **2**. The endocyclic P P bond distances (2.16 Å) and the P1 C1 bond distances (1.85 Å) are in the typical range of single bonds, the bond length of P2 C2 (1.71 Å) on the other hand indicates still significant double bond character. Both C O distances are in the typical range of a double bond (1.22 Å) and the Fe P bonds (2.25–2.27 Å) are longer compared to classical iron phosphine

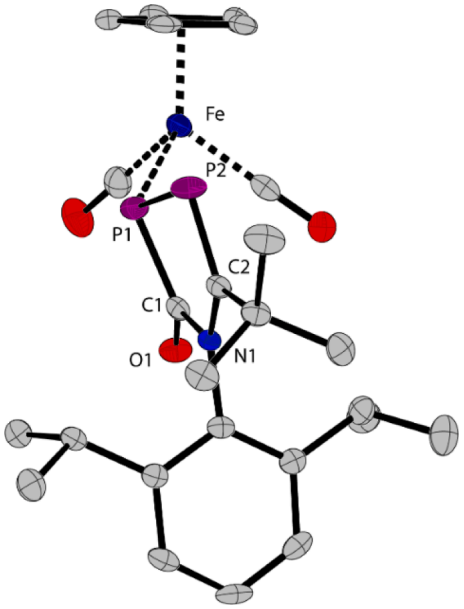

Fig. 3. Crystal structure of **3** emphasizing the pyramidal coordination sphere around P1. Anisotropic thermal displacement ellipsoids are shown at the 50% probability level. Hydrogen atoms are omitted for clarity. Interatomic distances (Å): Fe P1 2.2919(8), P1 P2 2.1458(11), P1 C1 1.814(3), P2 C2 1.715(3); Angles (°): P2 P1 Fe 115.32(4), C1 P1 Fe 109.52(9), C1 P1 P2 93.98(9).

interactions (c.f. Fe PPh_3 2.237 Å) [42] but little shorter compared to the ones in complex **3** [2.2919(8) Å]. The $^1J_{P,P}$ coupling constants for the two endocyclic phosphorus atoms decreased from 305.2 Hz and 239.6 Hz in **2** to only 123.8 Hz and 124.6 Hz in both iron complexes **4-syn** and **4-anti**. Under the assumption that the oxidation state at the iron centers is + 2, and the bridging phosphorus centers of two anionic coordinating azadiphospholide moieties donate a total of four electrons in the Fe_2P_2 ring, an 18-electron count is reached at every Fe center. The IR spectrum of the isolated product has only one but broad absorption band in the range of a metal carbonyl (ν_{CO} = 1938 cm^{-1}) and is significantly shifted to smaller wavenumbers compared to the structurally similar compound **VI** (2044, 2032, 1999, 1978 cm^{-1}) [43] (Scheme 4) indicating an increased electron density at the iron center and hence a stronger back donation to the carbonyl group.

DFT calculations of the five possible isomers of complex **4'** were also

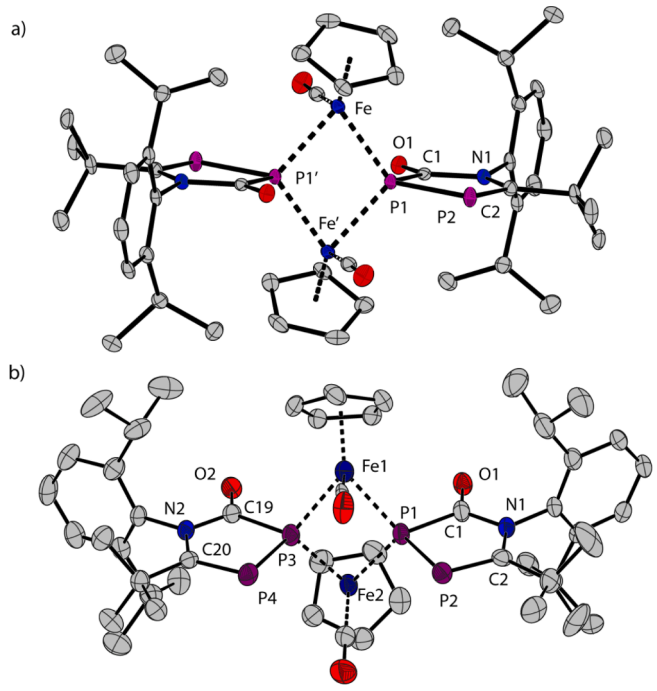

Fig. 4. Crystal structure of compound **4-anti** (a) and **4-syn** (b). Anisotropic thermal displacement ellipsoids are shown at the 50% probability level. Hydrogen atoms and solvent molecule are omitted for clarity reasons. **4-anti**: Both iron centers are identical in the solid state. Interatomic distances (Å): Fe1 Fe2 3.4785(6), Fe1 P1 2.2573(7), Fe1 P1 2.2447(7), P1 P2 2.1613(9), P1 C1 1.852(3), P2 C2 1.709(3), O1 C1 1.217(3), N1 C1 1.417(3), N1 C2 1.410(3). **4-syn**: Only one of the two diasteromers is shown. Interatomic distances (Å): Fe1 Fe2 3.4563(8), Fe1 P1 2.2557(14), Fe1 P3 2.2544(14), Fe2 P1 2.2603(14), Fe2 P3 2.2739(15), P1 P2 2.1639(17), P1 C1 1.852(5), P2 C2 1.704(5), O1 C1 1.224 (6), P3 P4 2.1614(18), P3 C19 1.855(5), P4 C20 1.711(4), O2 C19 1.217(5), fold angle Θ(Fe1 P1 Fe2 P3) = 20.6366(7) °.

performed, which arise from the *cis*, *trans* isomerism (*anti* or *syn* at the P centre and *cis* or *trans* at the Fe centre: *anti-trans*, *anti-cis*, *syn-trans* and two isomers of *syn-cis*) on a $[Fe_2(Cp)_2(\mu_2\text{-}\mathbf{1}')(CO)_2]$ model system, in which **1′** stands for a azadiphospholide where the *t*Bu and Dipp groups were replaced by Me. These isomers have rather similar relative energies and lie within an energy span of 3.0 kcal/mol, indicating no clear preference of any of these isomers. The bond lengths and the Wiberg bond indices for the relevant bonds such as Fe-P, P-P, Fe-C are very similar for all these isomers, and fit to those obtained in the solid state, for details see the Supporting information. Compared to the monomeric complex **3'**, the iron centres in all isomers of the dinuclear complexes **4'** are slightly less negatively charged (−1.17 e and −1.14 e in complexes **3'** and **4'**, respectively), while the P centres in **4'** carry higher charges (around + 0.70 e) than that in complex **3'** (+0.34 e), showing that the bridging P atoms are somewhat stronger electron donors. For comparison, an DFT optimization of the electronic structure of an dinuclear $[Fe_2(\mu_2\text{-}PMe_2)_2(Cp)_2(CO)_2]$ complex was performed in which the heterocycles were replaced by dimethyl phosphide ligands. The overall bonding features of this model complex are similar to those in **4'**. However, in $[Fe_2(\mu_2\text{-}PMe_2)_2(Cp)_2(CO)_2]$ the Fe centres bear even more negative charges (−1.20 e) and the Wiberg bond index of its Fe-P bond (0.77) indicates a stronger bond than in **4'** (Fe-P: 0.72 to 0.74 for the different isomers). As expected, these results suggest that the donor properties of the azadiphopholide anion are smaller than those of of dimethyl phosphide due to delocalization of the negative charge in the heterocycle.

In analogy to the reductive cleavage reaction between the bis(1-aza-3,4-diphospholyl) **2** and the Fe(I) complex $[Fe_2(Cp)_2(CO)_4]$ which led to the Fe(II) complex **3**, we tried to access a dinuclear Fe(I) complex by reacting **2** with an Fe(0) complex like $Fe_3(CO)_{12}$ as reductant. Both reactants were dissolved in a minimum amount of THF and were placed in a closed Young-flask to reflux for 6 h. The reaction mixture turned dark red and the ^{31}P NMR spectrum of the reaction mixture revealed the formation of two new sets of multiplet resonances. This leads to the assumption that again two stereoisomers were obtained which hints indeed to the formation of dinuclear complexes $[Fe_2(\mu_2\text{–}\mathbf{1})(CO)_6]$ comparable to the Fe(II) complexes **4-syn** and **4-anti**. One isomer shows a typical AA′XX′ spin system in the ^{31}P NMR spectrum ($^{31}P\{^1H\}$ NMR (CD_2Cl_2, 124.5 MHz): δ (ppm) = 69.9 (m), 80.9 (m) with $^1J_{AA'} = 226.2$ Hz, $^3J_{XX'} = 110.8$ Hz, $^1J_{AX} = 358.4$ Hz, $^2J_{AX'} = 24.2$ Hz). This spectrum is assigned to a C_{2v} symmetric isomer where the two tertiary butyl groups and the two CO units at each azadiphospholyl ring point to the same side with resepct to the central Fe—Fe bond and is therefore denominated **5-syn**. The second isomer shows four different phosphorus resonances coupling to each other (64.9 (ddd, $^1J_{P,P} = 331$ Hz, $^1J_{P,P} = 107$ Hz, $J_{P,P} = 17$ Hz), 78.2 (dd, $^1J_{P,P} = 331$ Hz, $J_{P,P} = 11$ Hz), 81.9 (dd, $^1J_{P,P} = 413$ Hz, $^1J_{P,P} = 107$ Hz, $J_{P,P} = 11$ Hz), 93.8 (ddd, $^1J_{P,P} = 413$ Hz, $J_{P,P} = 17$ Hz) which is indeed possible for a complex where the ^{t}Bu and CO groups point to opposite sides of Fe—Fe bond – named **5-anti** – and in which the four ^{31}P nuclei are inequivalent (see Scheme 5).

Recrystallization from diethyl ether yielded crystals of **5-syn** suitable for analysis by X-ray diffraction methods (see Fig. 5).

As already observed in the reaction between **2** and the dinuclear Fe (I) complex $[Fe_2(Cp)_2(CO)_4]$, iron centers become oxidized by one electron from Fe(0) to Fe(I) and formally insert into the central P—P bond of the tetraphosphane **2**. The two resulting azadiphospholide units take a bridging position between the two iron tricarbonyl fragments such that again a Fe_2P_2 ring is formed. In contrast to **4-syn** and **4-anti** this four-membered ring is now strongly folded (Θ = 100.717(2)°). The two iron centers in **5-syn** form a Fe—Fe bond with an interatomic distance of 2.5866(4) Å (Van der Waals radius for iron: 2.04 Å, Covalent radius for iron: 1.24 Å) [44] which almost one Å shorter than the Fe Fe distances in **4**. The Fe Fe bond distance is even shorter than the one observed in a dinuclear iron complex $[Fe_2(\mu\text{-nabip})_2(CO)_6]$ (2.6366(3) Å) which contains a bridging naphthalene-1,8-bis(phenylphosphido) (nabip) unit as rigid ligand. This compound was prepared in a similar way as **5-syn** and **5-anti** by reductively cleaving the P—P bond of the tricyclic precursor molecule naphthalene-1,8-diphenyldiphosphine with an Fe(0) carbonyl complex [45]. The CO stretching frequencies in $[Fe_2(\mu\text{-nabip})_2(CO)_6]$ (ν_{CO} = 2053, 2015, 1987, 1972 cm^{-1}) are very similar to the ones in complex **5-syn** (ν_{CO} = 2062, 2027, 1973 cm^{-1}) indicating similar electronic environments at the iron centers. Finally, we notice that in all dinuclear complexes reported in this paper, rather strong ^{31}P ^{31}P coupling contants (J = 107, 226 Hz, respectively) are observed (see Table 1) between the transannular P centers in the Fe_2P_2 rings in the range of regular ^1J coupling constants between singly bonded ^{31}P nuclei in diphosphanes, $R_2P—PR_2$, although the P P distances (2.81–2.86 Å) exclude any direct interaction. The results of DFT calculations (see Table 2 below) indicate that the structure of the azadiphospholide moiety in complex **5'** is very similar to those of complexes **4'**, and the Wiberg bond index of the Fe-Fe interaction is 0.38, being in accordance with the weakness of this bond. A significant difference between complexes **4'** and **5'** can be found in the partial charges of the iron centres, which are less negative for the former than for the latter (vide infra).

3. Disscussion and conclusion

One electron oxidation of the anionic 1,3,4-azadiphospholide $[\mathbf{1}]^-$ leads via a P-P coupling reaction to the formation of a neutral dimeric bis (1-aza-3,4-diphospholyl) **2** as product which contains a P_4-chain. This tetraphosphane **2** can be cleanly reconverted to salts M[**1**] containing the azadiphospholide as anion using alkali metals as reductants. This reversible redox process is accompanied by a prominent colour change from colourless $[\mathbf{1}]^-$ to dark yellow in **2**. Both compounds, $[\mathbf{1}]^-$ and **2**,

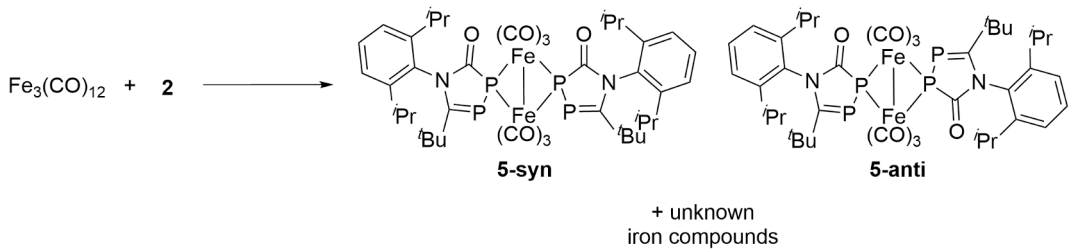

Scheme 5. Triiron dodecacarbonyl reacts with the dimer **2** to form the complexes **5-syn** and **5-anti**.

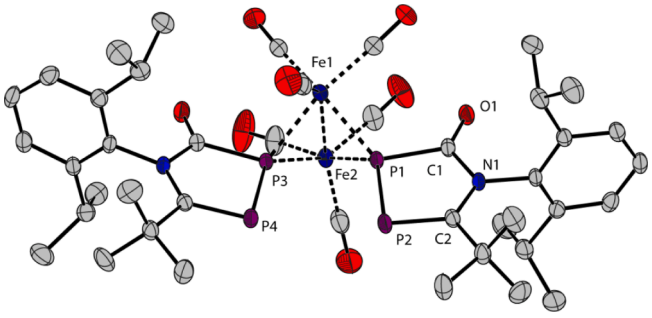

Fig. 5. Crystal structure of compound **5-syn**: The anisotropic thermal displacement ellipsoids are shown at the 50% probability level. Hydrogen atoms and two THF molecules are omitted for clarity reasons. Interatomic distances (Å): Fe1 Fe2 2.5866(4), P1 Fe1 2.2509(5), P1 Fe2 2.2244(6), P1 P2 2.1558(7), P1 C1 1.840(2), P2 C2 1.719(2), C1 O1 1.208(2),N1 C1 1.404(3), N1 C2 1.406(2), P3 Fe1 2.2273(6), P3 Fe2 2.2429(6), P3 P4 2.1528(7), P3 C24 1.8421(19), P4 C19 1.7182(19), N2 C24 1.402(2), N2 C19 1.410(2) Carbonyl C O 1.14 (averaged).

were applied as ligands in iron complexes. With Na[**1**] as reagent, these complexes are accessable via simple nucleophilic substitution reactions using a metal halide complex as precursor. With the tetraphosphane, metal complexes can be synthesized elegantly via redox reactions in which a reducing neutral metal precursor complex is employed. This method gives the desired products without any waste and also allows the synthesis of complexes with metals in unusual oxidation states such as the dinuclear Fe(I) complex $[Fe_2(\mu_2\text{–}\mathbf{1})_2(CO)_6]$ **5-syn/anti**. Recently related anionic phosphinine-2-olates, which contain an aromatic six-membered PC_5 ring with an anionic oxy-function adjacent to the λ^3,σ^2-P center in the ring were investigated as ligands in various Cu(I) and Au(I) complexes and η^1-coordination and μ_2-bridging coordination modes to the metal centers were established [46]. It was observed that the classical η^1-coordination mode is accompanied by a modest coordination shift to lower frequencies ($\Delta^{coord} \approx -30$ ppm) while the less usual μ_2-bridging coordination mode is indicated by a strong negative Δ^{coord}. Some coordination modes for an anionic 4-aza-1,2-diphospol-2-olate are shown in Fig. 6. Note that closely related descriptions have been made for related easily polarizable phosphorus heterocycles as ligands which also show that in dependence of the electronic structure of the ligand intermediate bonding situations between those shown in Fig. 6 are possible [47–50]. Note that the two possible terminal 2 electron coordination modes do not represent resonance structures but correspond to distinct electronic ground states in which in one case the coordination sphere around the bound P center is planar [2e terminal pl, see (a)] and in the other pyramidalized [2e terminal py, see (b)]. For the bridging mode, likewise several possibilities exist and two limiting cases are shown in Fig. 6: One in which the bridging phosphorus heterocycle acts as two electron donor [see (c)] and one in which it acts as 4 electron donor [see (d)]. While the latter has been frequently observed [46–54], the former is rare and there are only few complexes where this binding mode likely occurs. In the binuclear rhodium and iridium 2-pyridyl phosphinine (niphos) dications, $[Rh_2(nbd)_2(niphos)_2]^{2+}$ and $[Ir_2(1,5\text{-cod})_2(niphos)_2]^{2+}$ (nbd = norbornadiene, 1,5-cod = 1,5-cyclooctadiene), respectively, the bridging μ_2-phosphorus centers of the niphos ligand were assumed to be 2 electron donors [54]. Both complexes show a weakly negative Δ^{coord}. A second example is given by a Pd_3 cluster with bridging 2,4,6-triphenyl phosphinines [55] where notably the ^{31}P NMR resonance of the bridging ligand shows a positive Δ^{coord} of + 10 ppm to higher frequencies. Finally, a dinuclear Ru

Table 2
Selected Wiberg bond indices and partial NPA charges in electron at the BP86/cc-pVDZ level. These calculated data refer to model species in which the bulky DIP and *t*Bu groups have been replaced by Me.

	Na[1']	3'	4'-syn	4'-anti	5'-syn
P1 P2	1.17	1.05	0.95	0.96	0.98
P1 C1	1.27	0.99	0.89	0.89	0.89
C1 O	1.36	1.64	1.68	1.69	1.72
P2 *C2*	1.48	1.54	1.57	1.57	1.54
P1 Fe		0.75	0.74	0.74	0.76
Fe Fe			0.06	0.06	0.38
q(P1)	−0.25	0.35	0.71	0.71	0.69
q(C)	0.29	0.41	0.45	0.46	0.47
q(O)	−0.79	−0.42	−0.57	−0.57	−0.57
q(Fe)		−1.17	−1.15	−1.14	−1.88

Table 1
Averaged interatomic distances (Å) are extracted from the crystallographic data. The coupling constants are stated in Hz and have been measured from the ^{31}P NMR spectra. ATR-IR spectra were recorded on the Bruker alpha FT-IR of the powder under protective atmosphere.

	2-meso	2-rac	3	4-syn	4-anti	5-syn
P1 P2 [Å]	2.175	2.2328	2.146	2.1627	2.161	2.1543
P1 P3 [Å]	2.231	2.1699		2.8474	2.858	2.8100
P1 C1 [Å]	1.835	1.853	1.814	1.854	1.852	1.8431
P2 *C2* [Å]	1.709	1.717	1.715	1.708	1.709	1.719
Fe Fe [Å]	–	–	–	3.4563	3.478	2.5866
Fe1 P1 [Å]	–	–	2.292	2.2550	2.251	2.2391
O1 C1 [Å]	1.232	1.215	1.230	1.2221	1.217	1.208
$^1J_{P1,P2}$ [Hz]	311, 300 *		333	309	314	387
$^1J_{P1,P3}$ [Hz]	305, 240 *		–	125	138	55
νCO [cm^{-1}]	–		2021, 1990, 1966	1938£		2062, 2027, 2005, 1972

*) Coupling constant not assigned to a specific isomer. £) IR spectrum measured of the mixture of **4-syn** and **4-anti**.

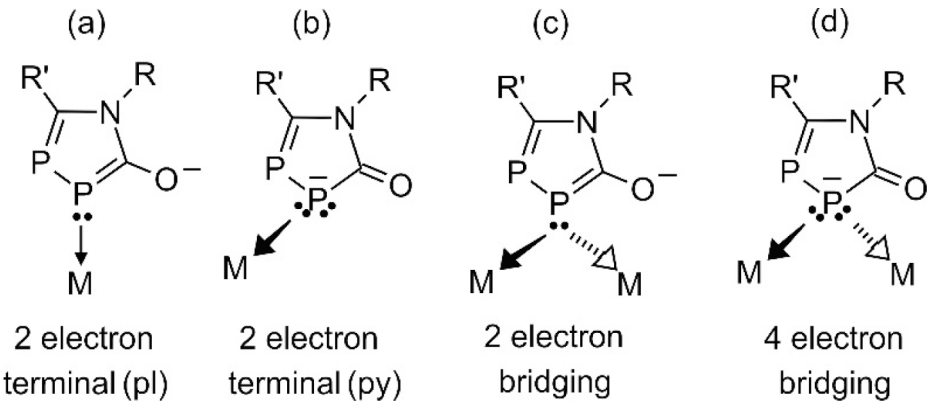

Fig. 6. Principal coordination modes of 1-aza-3,4-diphospholides $[\mathbf{1}]^-$.

complex containing a 2,2′-biphosphinine as bridging ligand contains for which no NMR data are available [56]. These results imply that complexes with a bridging phosphorus heterocycle as 2e donor preferably contain metal centers in low oxidation states (for a more detailed analysis of the bonding in such complexes, which can be described with 3-center-2-electron bonds further modulated by the perpendicular π -electron system in the heterocycle, see refs [48,49]). There are further few examples, where the structural data suggest that a neutral phosphinine acts as bridging two electron donor in Cu(I) [46,57,58] and Ag (I) [59] complexes. However, the ^{31}P NMR indicates that these structures are not retained in solution and the dinuclear complexes dissociate into classical η^1-phosphinine complexes in solution.

As the structures in Fig. 6 suggest, there are structural differences to be expected in dependence of the coordination mode of a 1-aza-3,4-diphospholide.

Notably, in all reactions reported in this study exclusively the phosphorus center adjacent to the carbonyl group in the P_2NC_2 ring is involved, which is in agreement with the fact that the HOMO has its largest coefficient at this phosphorus center P1. In Na[**1**], the ^{31}P nucleus P1 is observed at $\delta = 13.5$ ppm in a ^{31}P NMR spectrum while the other ^{31}P nucleus P2 embedded in the P—P2═C unit is observed at $\delta =$ 131.8 ppm. Upon coordination to a metal center in a terminal η^1-mode as in **3**, the ^{31}P resonance of P1 is strongly shifted to lower frequencies as expressed by the coordination shift $\Delta^{coord} = \{\delta$ (complex) – δ ($[\mathbf{1}]^-$ $\} =$ −58 ppm. This observation is in agreement with a rather strong pyramidalisation at P1 ($\Sigma^\circ = 318.9^\circ$) which indicates that a stereochemical active lone pair of electrons is formed when $[\mathbf{1}]^-$ is employed as ligand. A comparable observation was made when an anionic phosphinine-2-olate was coordinated to a $[Au(PPh_3)]^+$ fragment which likewise induced a Δ^{coord} of −50.7 ppm and a sum of bond angles of 351° at the P center was observed [46]. When the anionic azadiphospholide $[\mathbf{1}]^-$ takes a bridging position between two Fe(II) centers as in *syn/anti*-$[Fe_2(Cp)_2(\mu_2$–**1**$)(CO)_2]$ (**4-syn/anti**) an even stronger shift to lower frequencies is observed ($\Delta^{coord} \approx -92$ ppm) which likewise is in agreement with observations made with phosphinine-2-olates as μ_2-metal-bridging ligand in Cu(I) and Au(I) complexes [46]. Note that also the chemical shift of the other phosphorus nucleus in the ring, P2, is influenced by the coordination and shifted to lower frequencies although to a lesser extent.

A remarkable exception is seen in complexes **5-syn/anti** which contain two Fe(I) centers connected by a short Fe—Fe bond. Here, both ^{31}P nuclei show chemical shifts in the same range $\delta = 64.9$–93.8 ppm indicating that P1 is shifted by about + 60 ppm to higher frequencies while P2 is shifted by about −50 ppm to lower frequencies.

Table 1 summarizes selected physical data for all compounds which could be structurally characterized in this study **2-rac, 2-meso**, **3**, **4-syn**, **4-anti**, **5-syn**. As can be seen, the structural parameters of the 1-aza-3,4-diphospholide ring do not change much in **2-rac/meso** and **4-syn/anti**. The P1 P2 bond distances are long (>2.15 Å) as well as the P1 C1 distances within the P—C—O unit (>1.84 Å). But the C1 O1 distance is comparatively short. In combination, this indicates that in the tetraphosphane **2-rac/meso** and in the Fe(II) complexes **4-syn/anti** with a bridging azadiphospholide ring, the resonance form with a localized P$^-$—C═O unit, that is the carbonyl phosphide form, prevails. In iron complex **3,** which contains a terminal bound azadiphospholide, the shorter P1 P2 and P1 C1 bond distances in combination with a longer C—O bond indicate a larger contribution of the resonance structure with an oxido unit, P═C—O$^-$.

Table 2 lists selected Wiberg bond indices (WBIs) and partial NPA charges for Na[**1'**], **3'**, **4'-syn/anti**, and **5'-syn** for comparison. As can be seen, the WBIs for **4'** and **5'** as well as the partial charges at P1, C, and O are very similar and in accordance with the structural parameters which in combination indicate that the P1 C1 bond is best described as a single bond while the C O bond has high double bond character. Indeed, a comparison between the WBIs and NPA charges of Na[**1'**] and **3'** show, again in accordance with the bond distances discussed above, that in both the P1 P2 bond has a WBI > 1 while the C1 O bond has a slightly smaller WBI when compared to **4'-syn/anti** and **5'-syn** indicating a larger contribution of the oxido-resonance form shown in Fig. 6a to the electronic ground state.

Within the series of the iron complexes **3'**, **4'-syn/anti** and **5'**, the large negative charge of −1.88 e at the Fe(I) in **5'** is especially noteworthy which reflects its lower oxidation state. A comparison of the sum of the NPA charges at the CO (ca. + 0.3 e) and Cp^- ligand (ca. + 0.29 e) in the dinuclear complexes **4'-syn/anti** and **5'** shows that these are about the same in all complexes. The only significant difference is observed for the diazaphosphol ligands in **4'** which is less positively charged (+0.54 e) compared to **5'** (+0.74 e). This suggest that the diazaphospholide ligand in **5** is a slightly better electron donor that in **4**. One can therefore assume that the bridging-diazaphospholide in **4** is best described by a mixture of resonance structures (c) and (d) while in **5** form (d) prevails. With respect to the unusal ^{31}P NMR chemical shifts of the phosphorus nuclei, there is at present no straight-forward explanation but this may be caused by the unusual Fe—Fe bond in **5**.

4. Experimental

4.1. General considerations

All air- and moisture-sensitive manipulations were carried out using standard vacuum line Schlenk techniques or in an MBraun inert atmosphere dry-box containing an atmosphere of purified argon. THF was distilled from sodium benzophenone ketyl before use. THF-d_8 and C_6D_6 were purchased from Cambridge Isotope Laboratories and were distilled over potassium. The azadiphospholide Na[**1**] was synthesized according to literature procedures [22].

^{1}H NMR spectra were recorded on Bruker spectrometers operating at 300, 400 and 500 MHz, ^{13}C NMR at 75.4 MHz 100.6 MHz, ^{31}P NMR at 101.3, 121.5 and 162.0 MHz. All ^{1}H and ^{13}C NMR chemical shifts are reported relative to $SiMe_4$ using the ^{1}H (residual) and ^{13}C chemical shifts of the solvent as a secondary standard. ^{31}P spectra were externally referenced to an 85% solution of H_3PO_4 in H_2O. Peak widths at half heights (in Hz) are given for broad signals. Infrared spectra were collected on a Bruker-alpha FT-IR-spectrometer with the ATR measuring device. UV/Vis spectra were recorded on UV/vis/NIR lambda-19-spectrometer in a cell with a 1 or 2 mm path length. Elemental analyses were performed at the Mikrolabor of ETH Zürich.

Single crystals suitable for X-ray diffraction were coated with polyisobutylene oil in a dry-box, transferred to a nylon loop and then transferred to the goniometer of a Bruker X8 APEX2 diffractometer or on an Oxford Excalibur equipped with a molybdenum X-ray tube (λ = 0.71073 Å) and Sapphire 3 CCD-detector using CrysAlisPro [60]. Preliminary data was collected to determine the crystal system. The space group was identified and the data were processed using the Bruker SAINT + program and corrected for absorption using SADABS. The structures were solved using direct methods (SHELXS) [61–64] on OLEX2 [64] completed by Fourier synthesis and refined by full-matrix least-squares procedures. The rigid groups for the description of the disordered solvent molecules were obtained from the Idealized Molecular Geometry Library [65].

4.1.1. Preparation of the dimer 2

The azadiphospholide Na[**1**] (200 mg, 0.4 mmol) was dissolved in 4 mL of THF and was cooled down in an ice bath. C_2Cl_6 (50 mg, 0.2 mmol) was added as a solid to the reaction mixture. The mixture changed colour from colourless to dark yellow. The reaction mixture was stirred for 4 h and was then filtered through Celite. The volatiles were removed under reduced pressure. The product was stirred in 1 mL of hexane and filtered cold to obtain 115 mg of a yellow solid (84% yield). The hexane washing solution was placed in the freezer at −30 °C to yield single crystals suitable for X-ray analysis. MF: $C_{36}H_{52}N_2O_2P_4$, MW: 668.72 g/mol, EA[calc %]: C, 64.66; H, 7.84; N, 4.19; EA[found %]: C, 64.61; H, 7.82; N, 4.05; Absorption max in THF [λ_{max}]: 407 nm, 317 nm; MP: 184 °C; ^{31}P{^{1}H} NMR (CD_2Cl_2, 202.5 MHz, 263 K): δ (ppm) = Isomer 1; 75.4 (m), −39.2 (m) with $^{1}J_{AA'}$ = 305.2 Hz, $^{3}J_{XX'}$ = 34.4 Hz, $^{1}J_{AX}$ = 310.6 Hz, $^{2}J_{AX'}$ = 9.6 Hz Isomer 2; 74.3 (m) −48.1 (m), $^{1}J_{AA'}$ = 239.6 Hz, $^{1}J_{AX}$ = 300 Hz, $^{2}J_{AX'}$ = −9.5 Hz, $^{3}J_{XX'}$ = 0 Hz; ^{1}H NMR (CD_2Cl_2, 300 MHz): δ (ppm) = 1.00 (broad-d, J = 18.5 Hz, 6H, CH_3), 1.11 (s, 9H, CH_3 (^{t}Bu)) 1.20 (broad-d, J = 6.2 Hz, 6H, CH_3 (^{i}Pr)), 2.5–2.9 (m, 2H, CH (^{i}Pr)), 7.19 (broad-d, J = 7.7 Hz, 2H), 7.4 (t, J = 7.7 Hz, 1H); *Very broad signals, often two overlapping*: ^{13}C{^{1}H} NMR (CD_2Cl_2, 125.8 MHz): δ (ppm) = 22.3 (s, CH_3), 25.7 (s, CH_3), 29.5 (s, CH_3), 31.13 (not resolved) 42.6 (not resolved, Cq), 124.2 (s, CH_{arom}), 130.2 (s, CH_{arom}), 136.7 (s, CH_{arom}), 147.5 (broad, C_{arom}), 192.7 (broad, C═P), 210.6 (dd, not resolved, C═P); IR powder [cm^{-1}] : 2962, 2867, 1643, 1467, 1438, 1364, 1322, 1291, 1233, 1202, 1144, 1127, 801, 789, 740

4.1.2. Reduction of the dimer 2

A solution of the P_4-chain **2** in DME was divided and stored in two hermetically closed flasks, to one solution lithium was added and the mixture was stirred overnight. From both solution a sample (0.5 mL) was taken which was then enriched with the same volume of a PPh_3 stock solution. Quantitative ^{31}P NMR spectroscopy revealed full conversion back to anion Na[1]. ^{31}P NMR parameters were used from a validated method [66].

4.1.3. Preparation of 3

The azadiphospholide Na[**1**] (298 mg, 0.4 mmol) and FpI (110 mg, 0.4 mmol) were suspended in 15 mL of diethyl ether. The reaction turned immediately deep red. The solution was stirred for additional two hours. The reaction mixture was then filtered through Celite and concentrated to roughly 2 mL. The solution was placed in the freezer at −30 °C for 72 h to obtain a red solid contaminated with NaI. The product is dissolved in dichloromethane and filtered over Celite, the volatiles were removed to obtain 159 mg (78%) of a single crystalline strawberry red solid of the composition [FeCp(**1**)$(CO)_2$]. MF: $C_{25}H_{31}FeNO_3P_2$, MW: 511.32 g/mol; MP: 172 °C; EA[calc]: C, 58.73; H, 6.11; N, 2.74; EA [found]: C, 58.79; H, 6.13; N, 2.65; Absorption max [λ_{max}]: 515 nm; ^{1}H NMR (C_6D_6, 300 MHz): δ (ppm) = 7.2 (dd, J = 6.9, 8.4 Hz), 7.1 (d, J = 10.7 Hz), 4.3 (d, $^{3}J_{P,H}$ = 2.1 Hz, 5H, Cp), 3.0 (*sept*, J = 6.7 Hz), 1.3 (d, J = 6.7 Hz, 6H, CH_3), 1.3 (d, J = 2.2 Hz, 9H, CH_3), 1.2 (d, J = 6.7 Hz, 6H, CH_3). ^{31}P {^{1}H}NMR (C_6D_6, 124.5 MHz): δ (ppm) = 113.7 (d, $^{1}J_{P,P}$ = 332.4 Hz), −57.7 (d, $^{1}J_{P,P}$ = 332.8 Hz). ^{31}P NMR (C_6D_6, 124.5 MHz): δ (ppm) = 113.7 (d, $^{1}J_{P,P}$ = 332.3 Hz), −57.7 (d, $^{1}J_{P,P}$ = 332.4 Hz),. ^{13}C-{^{1}H} NMR (C_6D_6, 125.8 MHz): δ (ppm) = 212.9 (m, Carbonyl), 207.9 (d, J = 56.8 Hz), 199.8 (dd, J = 11.3, 74.6 Hz), 147.9 (s, CH_{arom}), 138.7 (d, J = 3.6 Hz), 129.4 (s, CH_{arom}), 123.6 (s, CH_{arom}), 85.0 (s, CH, Cp), 41.3 (dd, J = 2. 4, 16.7 Hz), 31.5 (dd, J = 3.6, 15.5 Hz, C_q (^{t}Bu)), 29.3 (s, CH_3 ^{t}Bu), 26.2 (s, CH, ^{i}Pr), 22.0 (s, CH_3, ^{i}Pr). IR[cm^{-1}] : 3106, 2961, 2870, 2021 (Fe-CO), 1990 (Fe-CO), 1966 (Fe-CO), 1578 (C═O), 1290, 1124, 846, 789, 616, 565

4.1.4. Alternative route to 3

The dimer **2** (67 mg, 0.1 mmol) and the $(CpFe(CO)_2)_2$ (21 mg, 0.06 mmol) were dissolved 5 mL of toluene and the reaction mixture was stirred overnight at 50 °C. The ^{31}P NMR spectrum of the reaction mixture contained the resonances matching the spectroscopical data for compound **3**.

4.1.5. Preparation of 4-syn and 4-anti

The Fp-adduct **3** (73.2 mg, 0.143 mmol) was dissolved in 2 mL of THF and 2 mL benzene. The reaction was stirred for 13 days at room temperature in a closed Schlenk-NMR tube in direct sunlight. The generated carbon monoxide pressure was released from time to time (note, the reaction time can be reduced to 3 h if a medium pressure mercury UV lamp is used.). The colour of the reaction mixture changed from strawberry red to dark yellow. After complete conversion the mixture was filtered through Celite and the solution was layered with hexanes and placed in the freezer at −30 °C for 72 h to obtain 57.5 mg (83%) of a yellow to red microcrystalline solid of the composition [{FeCp(**1**)(CO)}$_2$]. Single crystals for X-ray analysis were grown from an ether/benzene solution upon slow evaporation of the solvent. MF: $C_{48}H_{62}Fe_2N_2O_4P_4$; MW: 966.62 g/mol; MP: 120 °C (dec.); EA[calc]: C, 59.64; H, 6.47; N, 2.90; EA[found]: C, 59.00; H, 6.54; N, 2.67; Absorption max [λ_{max}]: 686 nm, 391 nm, shoulder at 401 nm. **4-syn** and **4-anti**; ^{31}P{^{1}H} NMR (THF, 121.5 MHz): δ (ppm) = 133.6 (m), −77.8 (m) with $^{1}J_{AA'}$ = 124.6 Hz, $^{3}J_{XX'}$ = 0 Hz, $^{1}J_{AX}$ = 308.7 Hz, $^{2}J_{AX'}$ = −15.8 Hz, ^{31}P{^{1}H}-NMR (THF, 121.5 MHz): δ (ppm) = 123.8 (m), −77.9 (m) with $^{1}J_{AA'}$ = 137.7 Hz, $^{3}J_{XX'}$ = 0 Hz, $^{1}J_{AX}$ = 314.4 Hz, $^{2}J_{AX'}$ = 4.8 Hz. Due to overlapping only ranges for the peaks in the ^{1}H and ^{13}C can be given. ^{1}H NMR (THF-d8, 400 MHz): δ (ppm) = 7.04–7.55 (m, CH_{arom}, 6H), [4.53, 4.35, 4.30, 4.24, 4.17, 4.26], s, C_5H_5, 10*H*), 2.9–2.5 (sept, overlap, CH, $^{1}J_{H,H}$ = 6.73 Hz, 4H), 1.3 – 0.9 (m, CH_3, overlap, 42H), ^{13}C NMR (THF-d8, 75.8 MHz): δ (ppm) = 147,5 (s, C_{arom}), 137.1 (s, C_{arom}), 129.5 (s, CH_{arom}), 123.7 (s, CH_{arom}), {80.3, 80.0, 79.8}(s, C_5H_5). IR cm^{-1} (powder): 2958, 2867, 1938, 1634, 1467, 1320, 1289, 1126, 1053, 1002, 880, 839, 820, 801, 789.

4.1.6. Preparation of 5-syn and 5-anti

The P_4-chain **2** (200 mg, 0.3 mmol) and $[Fe_3(CO)_{12}]$ (150 mg, 0.3 mmol) were dissolved in 10 mL THF. The reaction mixture was stirred in a closed Young capped Schlenk flask for 6 h at 80 °C. The mixture turned dark red. The volatiles were removed under reduced pressure. The product was extracted in 20 mL of hexane and was filtered through Celite. The hexane solution was concentrated to 10 mL and placed in the freezer to obtain 96 mg of red crystals. The mother liquor was concentrated to 5 mL to isolate another 64 mg of product. Total yield 160 mg (42%) of [{Fe(**1**)$(CO)_3$}$_2$]. Recrystallization from Et_2O yielded red

crystals suitable for X-ray analysis of **5-syn**: MF: $C_{42}H_{52}Fe_2N_2O_8P_4$; MW: 948.47 g/mol; MP: 170 °C decomposition; EA[calc]: C, 53.19; H, 5.53; N, 2.95; EA[found]: C, 53.29; H, 5.93; N, 2.88; Absorption max [λ_{max}]: 462 nm, shoulder at 372 nm; IR powder [cm^{-1}] : 2963, 2870, 2062, 2026, 2005, 1972, 1651, 1291, 1131. $^{31}P\{^1H\}$ NMR (CD_2Cl_2, 124.5 MHz): δ (ppm) = 69.9 (m), 80.9 (m) with $^1J_{AA'}$ = 226.2 Hz, $^3J_{XX'}$ = 110.8 Hz, $^1J_{AX}$ = 358.4 Hz, $^2J_{AX'}$ = 24.2 Hz. ^1H NMR (CD_2Cl_2, 300 MHz): δ (ppm) = 1.0 (d, J = 6.7 Hz, CH_3, ^{i}Pr, 12H), 1.2 (d, J = 6.7 Hz, CH_3, ^{i}Pr, 12H), 1.8 (s, CH_3, ^{t}Bu, 18H), 2.6 (sept, J = 6.7 Hz, ^{i}Pr, 4H), 7.2 (d, J = 7.7 Hz, 4H, H_{arom}), 7.4 (t, J = 7.7 Hz, 4H, H_{arom}). ^{13}C NMR (CD_2Cl_2, 125.8 MHz): δ (ppm) = 211.8 (m, CP), 209.2 (s, CO), 190.2 (m, CP), 174.4 (s, CH_{arom}), 136.7 (s, CH_{arom}), 130.4 (s, CH_{arom}), 124.3 (s, CH_{arom}), 31.0 (t, $J_{P,C}$ = 8.2 Hz), 29.6 (s, CH), 25.5 (s, CH3), 22.0 (s, CH3) **5-anti:** $^{31}P\{^1H\}$ NMR (THF, 124.5 MHz): δ (ppm) = 64.9 (ddd, $^1J_{P,P}$ = 330.7 Hz, $^1J_{P,P}$ = 106.9 Hz, $J_{P,P}$ = 16.8 Hz), 78.15 (dd, $^1J_{P,P}$ = 330.7 Hz, $J_{P,P}$ = 10.6 Hz), 81.9 (dd, $^1J_{P,P}$ = 413.2 Hz, $^1J_{P,P}$ = 106.9 Hz, $J_{P,P}$ = 10.6 Hz), 93.8 (ddd, $^1J_{P,P}$ = 413.2 Hz, $J_{P,P}$ = 16.8 Hz).

4.2. Theoretical Calculations

The computations were carried out with the Gaussian 09 suite of programs [67]. All structures were optimized using the BP86 and ωB97XD functionals combined cc-pVDZ basis set. Both methods show very similar results and only the results with the BP86 functional are thus discussed. At each of the optimized structures vibrational analysis was performed to check that the stationary point located is a minimum on the potential energy hypersurface (no imaginary frequencies were obtained). For NBO analysis the NBO 5.0 program was employed as implemented in Gaussian 09 [68]. The molecular orbitals were plotted with Avogadro program [69].

CRediT authorship contribution statement

Riccardo Suter: Investigation, Methodology, Visualization, Writing - original draft. **Robert J. Gilliard:** Investigation, Methodology. **Javad Iskandarov:** Formal analysis, Investigation. **Zoltan Benkő:** Formal analysis, Investigation, Writing - original draft. **Michael Wörle:** Formal analysis, Investigation, Validation. **Hansjörg Grützmacher:** Conceptualization, Supervision, Funding acquisition.

Declaration of Competing Interest

The authors declare that they have no known competing financial interests or personal relationships that could have appeared to influence the work reported in this paper.

Acknowledgements

This work was supported by the Swiss National Science Foundation (SNF) and the ETH Zurich, NKFIH PD 116329, János Bolyai Research Fellowship, Új Nemzeti Kiválóság Program ÚNKP-20-5-BME-317, NRDI Fund (TKP2020 IES, Grant No. BME-IE-NAT) based on the charter of bolster issued by the NRDI Office under the auspices of the Ministry for Innovation and Technology. We thank Réka Morkai and Erik Kertész for assistance.

Appendix A. Supplementary data

"CCDC 1474008, 1420588, 1483247, 1483250, 1483249, 1487674, 1483248 contain the supplementary crystallographic data for this paper. The data can be obtained free of charge from The Cambridge Crystallographic Data Centre via www.ccdc.cam.ac.uk/structures." Supplementary data to this article can be found online at https://doi.org/10.1016/j.ica.2021.120274.

References

[1] R.K. Bansal, N. Gupta, Sci. Synth. 13 (2004) 729–738.
[2] V. Caliman, P.B. Hitchcock, J.F. Nixon, J. Chem. Soc. Chem. Commun. (1995) 1661–1662.
[3] D. Heift, Z. Benkő, H. Grützmacher, Chem. – Eur. J. 20 (2014) 11326–11330.
[4] R. Bartsch, P.B. Hitchcock, J.F. Nixon, J. Chem. Soc. Chem. Commun. (1987) 1146–1148.
[5] R. Bartsch, D. Carmichael, P.B. Hitchcock, M.F. Meidine, J.F. Nixon, G.J.D. Sillett, J. Chem. Soc. Chem. Commun. (1988) 1615–1617.
[6] C. Heindl, S. Reisinger, C. Schwarzmaier, L. Rummel, A.V. Virovets, E. V. Peresypkina, M. Scheer, Eur. J. Inorg. Chem. 2016 (2016) 743–753.
[7] C. Heindl, E.V. Peresypkina, A.V. Virovets, V.Y. Komarov, M. Scheer, Dalton Trans. 44 (2015) 10245–10252.
[8] M.H. Araujo, D.A. Rajão, A.C. Doriguetto, J. Ellena, E.E. Castellano, P.B. Hitchcock, V. Caliman, J. Braz. Chem. Soc. 13 (2002) 555–558.
[9] N.S. Townsend, S.R. Shadbolt, M. Green, C.A. Russell, Angew. Chem. Int. Ed. 52 (2013) 3481–3484.
[10] M.M. Al-Ktaifani, W. Bauer, U. Bergsträsser, B. Breit, M.D. Francis, F. W. Heinemann, P.B. Hitchcock, A. Mack, J.F. Nixon, H. Pritzkow, M. Regitz, M. Zeller, U. Zenneck, Chem. – Eur. J. 8 (2002) 2622–2633.
[11] R. Bartsch, P.B. Hitchcock, J.F. Nixon, J. Organomet. Chem. 375 (1989) C31–C34.
[12] A.S. Ionkin, W.J. Marshall, B.M. Fish, A.A. Marchione, L.A. Howe, F. Davidson, C. N. McEwen, Eur. J. Inorg. Chem. 2008 (2008) 2386–2390.
[13] J. Su, B. Wang, D. Liu, L. Du, Y. Liu, J. Su, W. Zheng, Chem. Commun. 51 (2015) 12680–12683.
[14] C. Pi, Y. Wang, W. Zheng, L. Wan, H. Wu, L. Weng, L. Wu, Q. Li, P.V.R. Schleyer, Angew. Chem. Int. Ed. 49 (2010) 1842–1845.
[15] L. Wan, C. Pi, L. Zhang, W. Zheng, L. Weng, Z. Chen, Y. Zhang, Chem. Commun. (2008) 2266–2268.
[16] Y. Wang, W. Guo, D. Liu, Y. Yang, W. Zheng, Dalton Trans. 45 (2016) 899–903.
[17] W. Zheng, G. Zhang, K. Fan, Organometallics 25 (2006) 1548–1550.
[18] M. Zhao, W. Ma, X. Liu, W. Zheng, Inorg. Chim. Acta 437 (2015) 110–119.
[19] M. Mlatecek, L. Dostal, Z. Ruzickova, J. Honzicek, J. Holubova, M. Erben, Dalton Trans. 44 (2015) 20242–20253.
[20] M. Zhao, L. Wang, P. Li, X. Zhang, Y. Yang, W. Zheng, Chem. Commun. 51 (2015) 16184–16187.
[21] M. Zhao, L. Wang, X. Zhang, W. Zheng, Dalton Trans. (2016).
[22] R. Suter, Z. Benkő, H. Grützmacher, Chem. – Eur. J. 22 (2016) 14979–14987.
[23] R. Suter, Z. Benkő, M. Bispinghoff, H. Grützmacher, Angew. Chem. Int. Ed. Engl. 56 (2017) 11226–11231.
[24] F.F. Puschmann, D. Stein, D. Heift, C. Hendriksen, Z.A. Gal, H.-F. Grützmacher, H. Grützmacher, Angew. Chem. Int. Ed. 50 (2011) 8420–8423.
[25] G. Becker, W. Schwarz, N. Seidler, M. Westerhausen, Z. Anorg, Allg. Chem. 612 (1992) 72–82.
[26] R. Suter, Y.B. Mei, M. Baker, Z. Benkő, Z.S. Li, H. Grützmacher, Angew. Chem. Int. Ed. 56 (2017) 1356–1360.
[27] A.R. Jupp, J.M. Goicoechea, Angew. Chem. Int. Ed. 52 (2013) 10064–10067.
[28] J.M. Goicoechea, H. Grützmacher, Angew. Chem. Int. Ed. 57 (2018) 16968–16994.
[29] D. Heift, Z. Benkő, R. Suter, R. Verel, H. Grützmacher, Chem. Sci. 7 (2016) 6125–6131.
[30] H. Binder, B. Schuster, W. Schwarz, K.W. Klinkhammer, Z. Anorg, Allg. Chem. 625 (1999) 699–701.
[31] J. Geier, H. Ruegger, M. Woerle, H. Grützmacher, Angew. Chem. Int. Ed. 42 (2003) 3951–3954.
[32] J. Geier, J. Harmer, H. Grützmacher, Angew. Chem. Int. Ed. 43 (2004) 4093–4097.
[33] J.D. Masuda, A.J. Hoskin, T.W. Graham, C. Beddie, M.C. Fermin, N. Etkin, D. W. Stephan, Chem. – Eur. J. 12 (2006) 8696–8707.
[34] S. Gomez-Ruiz, R. Wolf, E. Hey-Hawkins, Dalton Trans. (2008) 1982–1988.
[35] P. Kilian, H.L. Milton, A.M.Z. Slawin, J.D. Woollins, Inorg. Chem. 43 (2004) 2252–2260.
[36] P. Kilian, S. Parveen, A.L. Fuller, A.M.Z. Slawin, J.D. Woollins, Dalton Trans. (2008) 1908–1916.
[37] P. Kilian, A.M.Z. Slawin, J.D. Woollins, Dalton Trans. (2006) 2175–2183.
[38] S. Parveen, P. Kilian, A.M.Z. Slawin, J.D. Woollins, Dalton Trans. (2006) 2586–2590.
[39] P. Wawrzyniak, A.L. Fuller, A.M.Z. Slawin, P. Kilian, Inorg. Chem. 48 (2009) 2500–2506.
[40] P. Pyykkö, M. Atsumi, Chem. – Eur. J. 15 (2009) 186–197.
[41] D. Carmichael, X.F. Le Goff, E. Muller, New J. Chem. 34 (2010) 1341–1347.
[42] A.G. Orpen, L. Brammer, F.H. Allen, O. Kennard, D.G. Watson, R. Taylor, J. Chem. Soc. Dalton Trans. (1989) S1–S83.
[43] A. Decken, F. Bottomley, B.E. Wilkins, E.D. Gill, Organometallics 23 (2004) 3683–3693.
[44] W.M. Haynes, CRC Handbook of Chemistry and Physics CRC Press, National Institute of Standards and Technology.
[45] Y. Teramoto, K. Kubo, S. Kume, T. Mizuta, Organometallics 32 (2013) 7014–7024.
[46] Y. Hou, Z. Li, Y. Li, P. Liu, C.-Y. Su, F. Puschmann, H. Grützmacher, Chem. Sci. 10 (2019) 3168–3180.
[47] F. Mathey, Coord. Chem. Rev. 137 (1994) 1–52.
[48] D. Gudat, Coord. Chem. Rev. 163 (1997) 71–106.
[49] D. Gudat, Top. Curr. Chem. 232 (2004) 175–212.
[50] P. Le Floch, Coord. Chem. Rev. 20 (2006) 627–681.
[51] S.E. Thwaite, A. Schier, H. Schmidbaur, Inorg. Chim. Acta 357 (2004) 1549–1557.
[52] M.J. Bakker, F.W. Vergeer, F. Hartl, P. Rosa, L. Ricard, P. Le Floch, M.J. Calhorda, Chem. Eur. J. 8 (2002) 1741–1752.

[53] M.J. Bakker, F.W. Vergeer, F. Hartl, K. Goubitz, J. Fraanje, P. Rosa, P. Le Floch, Eur. J. Inorg. Chem. (2000) 843–845.
[54] B. Schmid, L.M. Venanzi, T. Gerfin, V. Gramlich, F. Mathey, Inorg. Chem. 31 (1992) 5117–5122.
[55] M.T. Reetz, E. Bohres, R. Goddard, M.C. Holthausen, W. Thiel, Chem. Eur. J. 5 (1999) 2101–2108.
[56] P. Rosa, L. Ricard, F. Mathey, P. Le Floch, Organometallics 19 (2000) 5247–5250.
[57] X. Chen, Z. Li, Y. Fan, H. Grützmacher, Eur. J. Inorg. Chem. (2016) 633–638.
[58] Y. Mao, K.M.H. Lim, Y. Li, R. Ganguly, F. Mathey, Organometallics 32 (2013) 3562–3565.
[59] M.H. Habicht, F. Wossidlo, T. Bens, E.A. Pidko, C. Müller, Chem. Eur. J. 23 (2018) 944–952.
[60] CrysAlisPro 1.171.40.67a (Rigaku Oxford Diffraction, 2019).
[61] G.M. Sheldrick, Acta Crystallogr. A 64 (2008) 112–122.
[62] G.M. Sheldrick, Acta Crystallogr. C 71 (2015) 3–8.
[63] G.M. Sheldrick, Acta Crystallogr. A 71 (2015) 3–8.
[64] O.V. Dolomanov, L.J. Bourhis, R.J. Gildea, J.A.K. Howard, H. Puschmann, J. Appl. Crystallogr. 42 (2009) 339–341.
[65] I.A. Guzei, J. Appl. Crystallogr. 47 (2014) 806–809.
[66] D. Heift, Z. Benkő, H. Grützmacher, Dalton Trans. 43 (2014) 831–840.
[67] M. J. Frisch, G. W. Trucks, H. B. Schlegel, G. E. Scuseria, M. A. Robb, J. R. Cheeseman, G. Scalmani, V. Barone, B. Mennucci, G. A. Petersson, H. Nakatsuji, M. Caricato, X. Li, H. P. Hratchian, A. F. Izmaylov, J. Bloino, G. Zheng, J. L. Sonnenberg, M. Hada, M. Ehara, K. Toyota, R. Fukuda, J. Hasegawa, M. Ishida, T. Nakajima, Y. Honda, O. Kitao, H. Nakai, T. Vreven, J. A. Montgomery Jr, J. E. Peralta, F. Ogliaro, M. Bearpark, J. J. Heyd, E. Brothers, K. N. Kudin, V. N. Staroverov, R. Kobayashi, J. Normand, K. Raghavachari, A. Rendell, J. C. Burant, S. S. Iyengar, J. Tomasi, M. Cossi, N. Rega, J. M. Millam, M. Klene, J. E. Knox, J. B. Cross, V. Bakken, C. Adamo, J. Jaramillo, R. Gomperts, R. E. Stratmann, O. Yazyev, A. J. Austin, R. Cammi, C. Pomelli, J. W. Ochterski, R. L. Martin, K. Morokuma, V. G. Zakrzewski, G. A. Voth, P. Salvador, J. J. Dannenberg, S. Dapprich, A. D. Daniels, Ö. Farkas, J. B. Foresman, J. V. Ortiz, J. Cioslowski and D. J. Fox, Gaussian 09, Revision E.01, Gaussian, Inc., Wallingford CT, 2013.
[68] NBO 5.0. E. D. Glendening, J. K. Badenhoop, A. E. Reed, J. E. Carpenter, J. A. Bohmann, C. M. Morales, and F. Weinhold, Theoretical Chemistry Institute, University of Wisconsin, Madison (2001).
[69] https://avogadro.cc/.